Investigation of the Impact Properties of Reactive Powder Concrete Containing Nano-Silica and Reinforced with Fibers under Repeated Drop-Weight Impact

Kiana ZanganehZadeh[1], Morteza Jamshidi*[2]

1.PhD student, Department of Civil Engineering, Chalus Branch, Islamic Azad University, Chalus, Iran.
2.Assistant Professor, Department of Civil Engineering, Chalus Branch, Islamic Azad University, Chalus, Iran (Corresponding author).

*** Corresponding author email address**: Jamshidi.iauc@gmail.com

Received: 2024-10-01 **Reviewed:** 2024-10-20 **Revised:** 2024-11-01 **Accepted:** 2024-11-27 **Published:** 2025-06-29

Abstract

Given the increasing demand for high-performance and sustainable construction materials, reactive powder concrete (RPC) has attracted significant attention from researchers due to its exceptional mechanical properties. In this study, the interactive effects of nano-silica (at 0%, 0.5%, and 1% by weight of cement), fiber type (steel and polypropylene), fiber content (0%, 1%, and 2% by volume), and curing method on the impact resistance of RPC were investigated. RPC samples were produced with various nano-silica and fiber contents and subjected to three different curing methods: standard moist curing for 28 days, thermal curing in hot water at 90°C for 2 and 5 days followed by standard moist curing until 28 days of age. The results of the drop-weight impact tests showed that steel fibers significantly improved the initial and final impact resistance of RPC, whereas polypropylene fibers had a lesser effect on these parameters. Additionally, the incorporation of nano-silica and thermal curing marginally enhanced the impact performance of RPC. Statistical analysis of the data using the two-parameter Weibull distribution indicated that this distribution is a suitable model for describing the failure behavior of RPC under impact loading.

Keywords: *Impact resistance, Reactive Powder Concrete (RPC), Nano-silica, Fibers, Weibull distribution.*

How to cite this article:

ZanganehZadeh K, Jamshidi M. (2025). Investigation of the Impact Properties of Reactive Powder Concrete Containing Nano-Silica and Reinforced with Fibers under Repeated Drop-Weight Impact. Management Strategies and Engineering Sciences, 7(2), 28-42.

1. Introduction

In today's world, rapid transformations are occurring, and civil engineering plays a crucial role in providing the foundation for current advancements. Concrete and concrete technology have also experienced significant progress in alignment with these changes [1]. Concrete is the second most widely used material globally after water. This widespread use is due to the abundant availability of concrete components and the relatively easier technology required for its preparation compared to other construction materials. The main advantages of concrete that contribute to its extensive use in the construction industry include the relatively low cost of its constituent materials, versatility in shape, ease of preparation, and desirable compressive strength [2, 3].

On the other hand, with the increasing construction of high-rise structures in recent years and the rising costs of maintenance and rehabilitation, researchers have intensified their efforts to develop concrete with desirable mechanical properties [4-6]. One of the approaches to achieving this goal is reducing concrete porosity, which has been the focus of many researchers. The result of these efforts initially led to the introduction of high-performance concrete (HPC), followed by the development of reactive powder concrete (RPC) in France in the early 1990s [7]). RPC is classified under ultra-high-performance concrete (UHPC), and its outstanding mechanical properties, such as high compressive and tensile strength, high energy absorption, low shrinkage, and low permeability, have garnered increasing attention [8].

The high energy absorption of RPC prevents collapse under cyclic and seismic loads. Moreover, the role of fibers in RPC is similar to that of reinforcement bars at the micro-level. Thus, the presence of fibers enhances the shear and tensile strength of this concrete, enabling the partial or complete elimination of flexural and shear reinforcements. The incorporation of fibers delays the formation of micro-cracks and controls their width [9]. This reduction in cracking minimizes deformation and deflection of structural elements under service loads.

Given the favorable mechanical properties of RPC, its application is expanding across various industries, including construction, oil, nuclear energy, and military sectors. Structures made with RPC have lower maintenance costs throughout their lifespan due to the high durability of this concrete. However, research in recent years has shown that RPC exhibits brittle and explosive failure behavior, which poses a significant limitation to its application [10]. Therefore, the use of fibers can mitigate this deficiency. Adding fibers to concrete can improve mechanical properties, increase energy absorption, and prevent crack propagation [3].

Additionally, short and discrete fibers can delay the propagation of impact-induced cracks. This effect is due to the fibers acting as bridges across cracks, preventing their expansion. Fiber bridging enhances concrete integrity and increases its flexural and tensile deformations [11]. The most commonly used fibers for improving concrete properties are steel fibers. However, other fibers, such as polypropylene fibers, also positively contribute to crack reduction and control in concrete. Furthermore, fibers can enhance the durability of concrete [12].

Ju et al. (2018) conducted an experimental study on the mechanical properties of RPC reinforced with polypropylene fibers. This study experimentally evaluated the effects of embedded polypropylene fibers on mechanical properties such as compressive strength, tensile strength, flexural strength, ductility, and fracture energy of RPC. Scanning electron microscopy (SEM) was also used to characterize the microstructure of fiber-reinforced RPC. The experimental results indicated that the addition of PP fibers with a volume fraction of less than 0.3% had negligible effects on the mechanical properties of RPC. The addition of PP fibers with a volume fraction between 0.3% and 0.9% improved mechanical strength and fracture performance. However, increasing the fiber volume fraction to 0.9% resulted in a slight reduction in all measured mechanical properties of fiber-reinforced RPC.

Shang et al. (2022) conducted a study titled Investigating Mechanical Properties and Microstructure of Reactive Powder Concrete Blended with Sulfoaluminate Cement. In this study, superabsorbent polymers, expansive agents, and shrinkage-reducing agents were used to improve the shrinkage performance of ultra-high-performance concrete (UHPC). The study results indicated that the addition of SAC significantly improved the compressive strength of RPC, particularly the early strength. Specifically, using SAC at 8% by weight resulted in an 871.4% increase in compressive strength and a 600% improvement in tensile strength after 8 hours of curing [13].

In this study, to evaluate the interactive effects of various factors on the impact behavior of reactive powder concrete (RPC), samples with different compositions of nano-silica (0%, 0.5%, and 1% by weight of cement) and steel and polypropylene fibers (0%, 1%, and 2% by volume) were

fabricated. These samples underwent three different curing methods, including standard moist curing, 2-day thermal curing, and 5-day thermal curing. To assess the impact resistance of the samples, repeated drop-weight impact tests were conducted in accordance with ACI C544 standards. Parameters such as initial crack resistance, final resistance, and energy absorption were measured. Statistical analysis of the data was performed using the two-parameter Weibull distribution to model the failure behavior of RPC under impact loading.

2. Experimental Program

2.1. Materials

In this study, Type II Portland cement was used in accordance with ASTM C150 standards [14]. The physical and chemical properties of this cement are presented in Table 1. Fine aggregates consisted of sand passing through a No. 30 sieve with a specific gravity of 2.7 g/cm³. Silica fume with a bulk density of 2.2 g/cm³, a specific surface area of 15 to 20 m²/g, and a purity of 92% was utilized. More than 80% of silica fume particles had a size of less than 1 micrometer, with an average particle size ranging from 0.3 to 0.6 micrometers. Additionally, nano-silica with an average particle diameter of 60 to 70 nanometers, a bulk density of 0.08 to 0.10 g/cm³, and a specific surface area of 160 m²/g was employed.

X-ray diffraction (XRD) analysis revealed that quartz was the predominant phase in silica fume (Figure 1). The XRD results also indicated the predominantly amorphous nature of nano-silica, with minor crystalline phases such as cristobalite and tridymite. The broadening of the XRD peaks in the nano-silica sample was attributed to the small crystallite size of the nanoparticles. Fourier-transform infrared spectroscopy (FTIR) analysis, shown in Figure 2, confirmed the presence of hydroxyl groups on the surface of silica nanoparticles. Scanning electron microscopy (SEM) images demonstrated that the silica nanoparticles exhibited irregular shapes and a non-uniform particle size distribution (Figure 3).

In this study, steel fibers with a length of 50 mm and a diameter of 0.8 mm, as well as polypropylene fibers with a length of 6 mm, were used as reinforcement (Table 2 and Figure 4). To improve the workability of the mixtures, a superplasticizer under the trade name Dezobuild D50 was added.

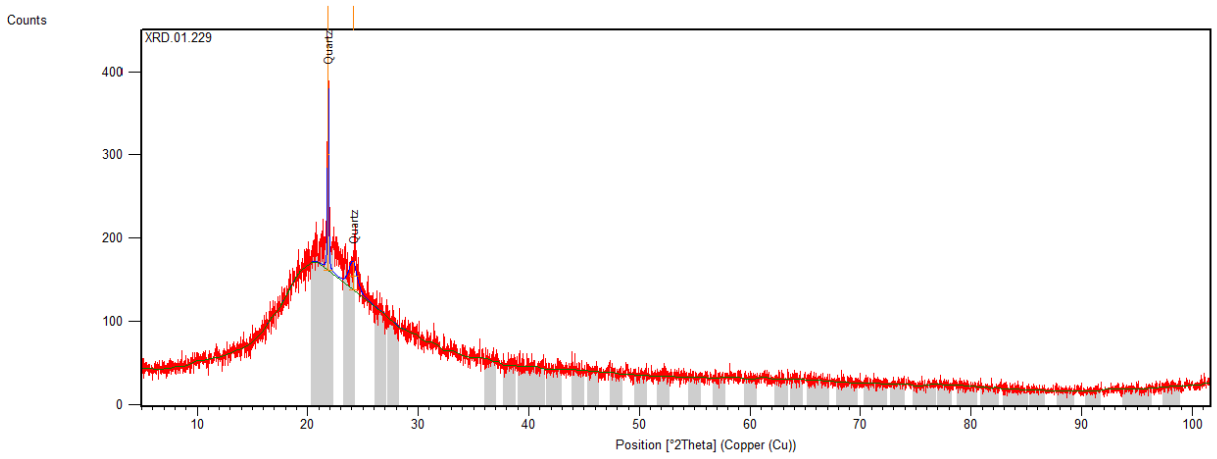

Figure 1. XRD analysis of nano-silica particles.

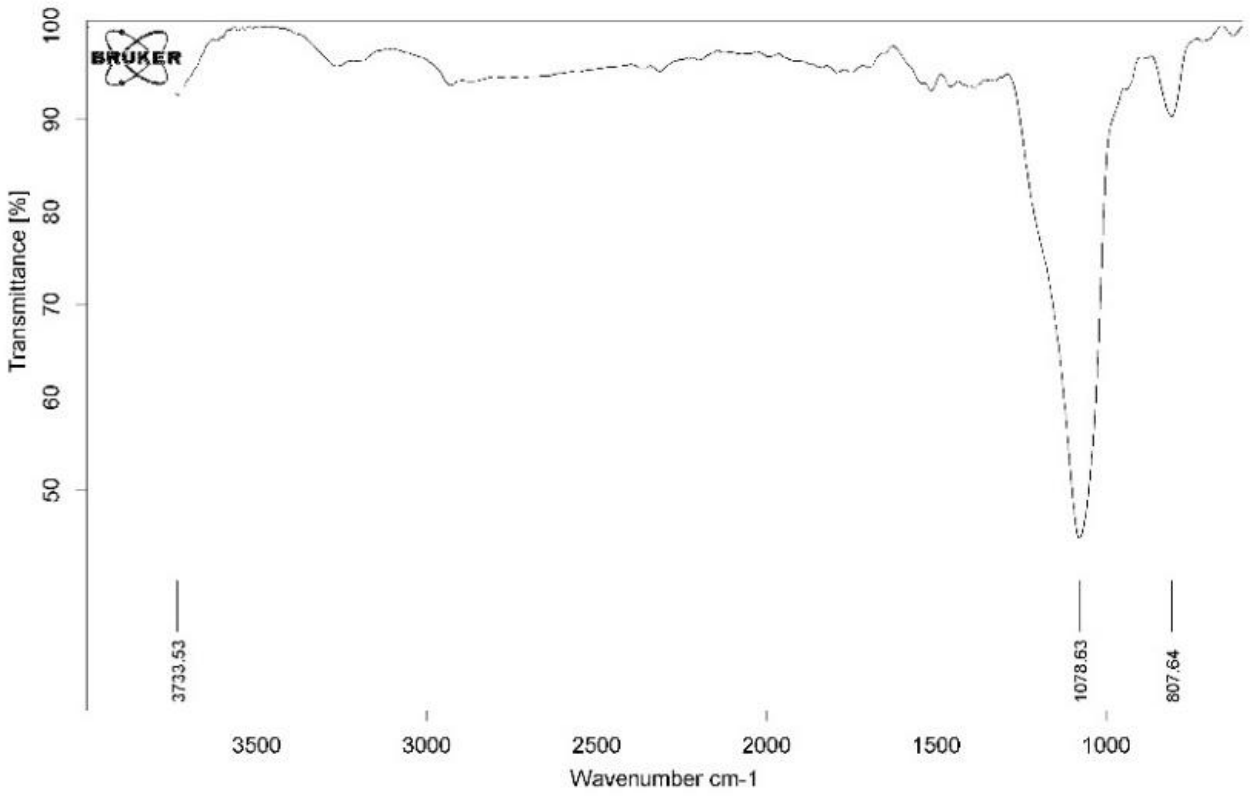

Figure 2. FTIR analysis of nano-silica particles.

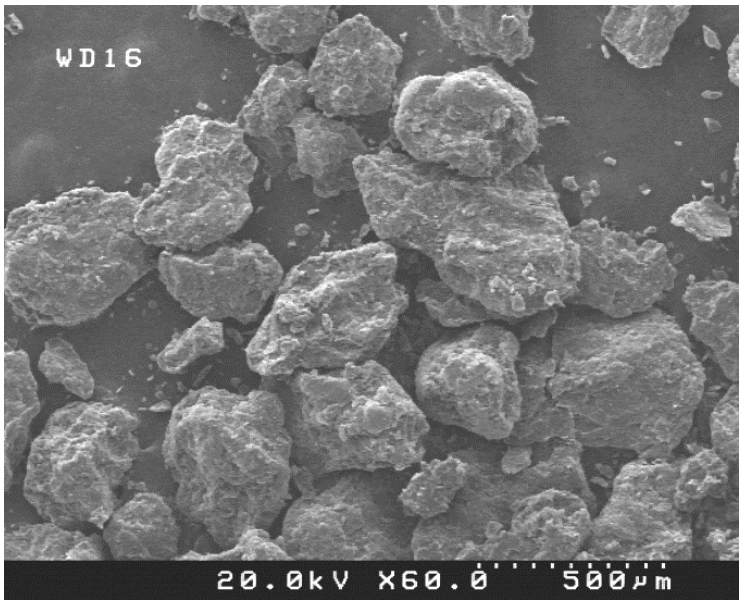

Figure 3. SEM image of nano-silica particles.

Figure 4. Fibers used in the study: (a) steel fibers and (b) polypropylene fibers.

Table 1. Chemical composition and physical properties of OPC.

**Chemical Properties (weight %) **	OPC
SiO_2	21.1
Al_2O_3	4.37
Fe_2O_3	3.88
MgO	1.56
K_2O	0.52
Na_2O	0.39
CaO	63.33
C_3S	51
C_2S	22.7
C_3A	5.1
C_4AF	11.9
Physical Properties	OPC
Specific Gravity (g/cm^3)	3.1
Specific Surface Area (cm^2/g)	3000

Table 2. Properties of steel and polypropylene fibers.

Properties	Steel Fibers	Polypropylene Fibers
Length (cm)	5	0.6
Diameter (cm)	0.08	-
L/D Ratio	62.5	-
Density (kg/m^3)	7850	910
Modulus of Elasticity (MPa)	200	3.5

2.2. Mix Designs and Sample Preparation

The mix designs used for sample preparation in this study are presented in Table 3. In these mix designs, nano-silica was incorporated at three levels: 0%, 0.5%, and 1% by weight of cement. Additionally, steel and polypropylene fibers were added at three volume fractions: 0%, 1%, and 2%. All other material quantities remained constant across the mix designs. It should be noted that the samples produced using these mix designs were subjected to three different curing methods.

Initially, the materials were dry-mixed for 10 minutes. Then, 90% of the water along with half of the superplasticizer was added and mixed for an additional four minutes. Finally, the remaining water and superplasticizer were added, and mixing continued for another four minutes. To prevent fiber balling, fibers were gradually introduced during the final mixing stage, and the mixing process continued until a visually homogeneous mixture was achieved.

Table 3. Mix Designs.

Mix Design	Cement (kg/m³)	Aggregate (kg/m³)	Water (kg/m³)	Silica Fume (kg/m³)	Nano-Silica (kg/m³)	Superplasticizer (kg/m³)	Steel Fiber (%)	Polypropylene Fiber (%)
M1	930	810	170.1	224	0	16.2	0	0
M2	930	810	170.1	224	0	16.2	1	0
M3	930	810	170.1	224	0	16.2	2	0
M4	930	810	170.1	224	0	16.2	0	1
M5	930	810	170.1	224	0	16.2	0	2
M6	930	810	170.1	224	4.05	16.2	0	0
M7	930	810	170.1	224	4.05	16.2	1	0
M8	930	810	170.1	224	4.05	16.2	2	0
M9	930	810	170.1	224	4.05	16.2	0	1
M10	930	810	170.1	224	4.05	16.2	0	2
M11	930	810	170.1	224	8.1	16.2	0	0
M12	930	810	170.1	224	8.1	16.2	1	0
M13	930	810	170.1	224	8.1	16.2	2	0
M14	930	810	170.1	224	8.1	16.2	0	1
M15	930	810	170.1	224	8.1	16.2	0	2

2.3. Curing Methods

To investigate the effect of curing methods on the properties of reactive powder concrete (RPC), the prepared samples were subjected to three different curing regimes. All samples were demolded after one day.

In the first curing method, the samples were immediately placed in a water tank at 20°C for 28 days. In the second and third curing methods, the samples were placed in hot water at 90°C for 2 and 5 days, respectively, and then transferred to a water tank at 20°C until reaching the age of 28 days.

3. Experimental Procedures

The compressive strength of the mixtures was evaluated at 28 days according to ASTM C39 standards [15] using three cubic specimens from each mix. The test was conducted using a digital compression machine with a capacity of 1000 kN, applying force at a rate of 0.3 N/mm².s.

The impact resistance test was performed using a repeated drop-weight impact method based on the procedure recommended by ACI C544 (ACI Committee 544, 1988). Figure 5 illustrates the details of the apparatus used for this test. In this test, disc-shaped specimens were placed inside the device, and a hammer weighing 4.45 kg was repeatedly dropped from a height of 457 mm onto a 63.5 mm steel ball positioned on the specimen surface.

The test results included the number of blows required to cause the first visible crack, the number of blows to cause ultimate failure, and the energy absorbed by the specimen. The impact energy per blow was calculated using the following equations:

1) $H = (gt^2)/2$

2) $V = gt$

3) $U = (WV^2)/2g$

Where:

- H is the drop height of the hammer (457 mm),
- g is the gravitational acceleration (9820 mm/sec²),
- t is the drop time per blow.

Using the given data, the hammer drop time per blow was calculated as 0.3052 seconds. According to the velocity equation, the hammer impact velocity at contact was determined to be 2994.01 mm/sec. Based on the calculated values and the energy equation, the impact energy per blow was determined to be 20.345 J. The total energy absorbed by the specimen was calculated by multiplying the number of blows by this value.

This test was conducted on concrete disc specimens prepared from all 15 mix designs under investigation.

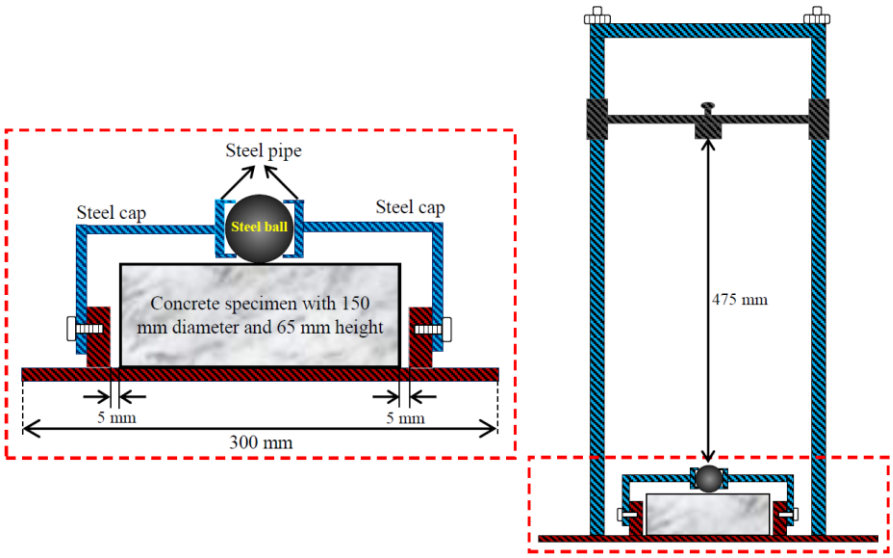

Figure 5. Details of the drop-weight impact test apparatus.

4. Analysis of Results

4.1. Compressive Strength

In this experiment, 45 cubic specimens from 15 mix designs and three curing methods were evaluated. Figure 6 presents the results of this test in terms of MPa. As observed from the results, the lowest compressive strength corresponds to mix design M1, which serves as the control mix, while the highest compressive strength is achieved by mix design M12, which contains 1% nano-silica and 1% steel fibers. The compressive strength of mix design M1 for curing methods 1, 2, and 3 was 71, 87, and 105 MPa, respectively. In contrast, the compressive strength of mix design M12 for the same curing methods was 121, 161, and 162 MPa, respectively. These results indicate the positive impact of thermal curing. Specifically, in mix design M1, using 2-day thermal curing increased the compressive strength from 71 MPa to 87 MPa, representing a 23% improvement. Furthermore, applying 5-day thermal curing raised the compressive strength to 105 MPa, which corresponds to a 48% increase compared to curing method 1 (without thermal curing) and a 16% increase compared to curing method 2 (2-day thermal curing). The positive effect of thermal curing can be attributed to its role in enhancing the hydration process and consequently increasing the strength of the concrete [16].

Additionally, a comparison between fiber-free mix designs and those reinforced with steel and polypropylene fibers suggests that incorporating an appropriate amount of steel fibers can enhance compressive strength performance. However, excessive fiber content may have an adverse effect, leading to a reduction in compressive strength. As evident from the results, comparing mixes M1, M2, and M3—containing 0%, 1%, and 2% steel fibers, respectively—confirms this observation. The fiber-free mix (M1) achieved a compressive strength of 71 MPa, while the addition of 1% steel fibers increased the strength to 74 MPa. However, increasing the steel fiber content to 2% reduced the compressive strength to 68 MPa. Thus, adding 1% steel fibers resulted in a 4% increase, while adding 2% led to a 4% decrease in compressive strength compared to the control mix (without fibers). A similar trend is observed in other mixes containing steel fibers compared to their fiber-free counterparts. The reason behind this is that an optimal fiber content can enhance matrix cohesion, preventing the formation and propagation of microcracks, thereby improving compressive strength. Conversely, excessive fiber content can create voids within the matrix, reducing compressive strength. Therefore, it can be concluded that the addition of fibers in optimal quantities positively affects the compressive strength of RPC, whereas excessive amounts have a detrimental impact [17, 18].

Furthermore, the mix designs containing polypropylene fibers indicate that these fibers do not significantly affect the compressive strength of the mixes. Instead, their influence is primarily on the durability properties of concrete rather than its mechanical properties [19].

On the other hand, the results of mixes containing nano-silica demonstrate its considerable impact on compressive strength. Comparing the control mix (without nano-silica) with mixes containing 0.5% and 1% nano-silica confirms

this effect. The control mix (without fibers and nano-silica) achieved compressive strengths of 71, 87, and 105 MPa for curing methods 1, 2, and 3, respectively. In contrast, mix M6 (without fibers and containing 0.5% nano-silica) achieved compressive strengths of 91, 122, and 131 MPa for the same curing methods. These results indicate that the use of 0.5% nano-silica increased compressive strength by 28%, 29%, and 20% compared to the control mix for curing methods 1, 2, and 3, respectively.

Further analysis of the compressive strength of mixes containing 1% nano-silica reveals that higher nano-silica content results in greater improvements. As shown in the results, mix M11 (without fibers and containing 1% nano-silica) achieved compressive strengths of 109, 144, and 154 MPa for curing methods 1, 2, and 3, respectively. These results indicate a 19%, 18%, and 18% increase in compressive strength compared to the 0.5% nano-silica mix and a 54%, 66%, and 47% increase compared to the control mix (without nano-silica).

Thus, it can be inferred that even small amounts of nano-silica can significantly enhance compressive strength. Moreover, the effect of nano-silica is consistent across all curing methods, indicating that changes in curing methods did not significantly alter the impact of nano-silica on compressive strength. The exceptionally high specific surface area and pozzolanic properties of nano-silica improve cement matrix reactivity and enhance performance in compressive strength tests [20, 21].

The interaction between the two parameters—fiber content and nano-silica dosage—resulted in the best performance in the compressive strength test. The highest compressive strength was achieved with the mix design containing 1% steel fibers and 1% nano-silica under curing method 3 (5-day thermal curing), with a compressive strength of 162 MPa.

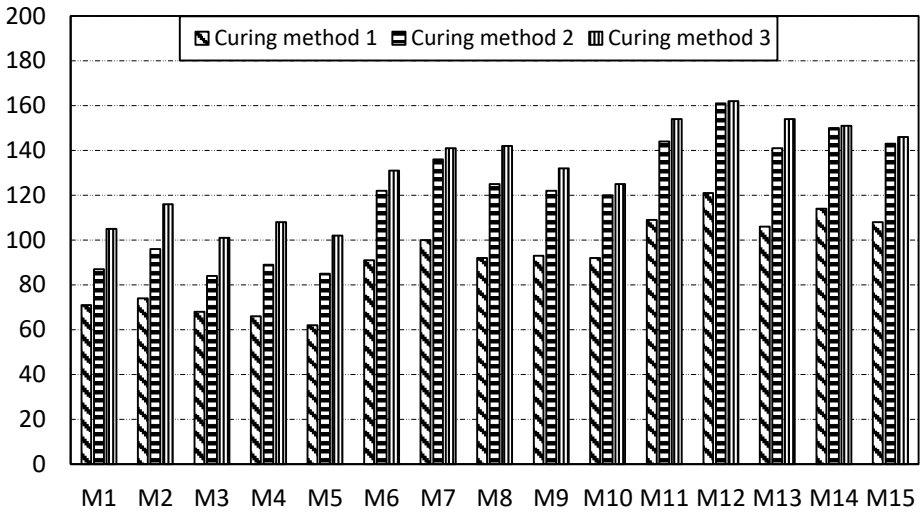

Figure 6. Compressive strength test results.

4.2. Impact Resistance

4.2.1. First Crack Impact Resistance

The number of blows required to initiate the first visible crack in the specimens was recorded, and based on this, the energy absorbed by the samples was calculated. The results for this parameter, measured in kilojoules (kJ), for the 45 evaluated specimens are presented in Figure 7. The results of the first crack resistance parameter indicate very poor performance for the samples produced with fiber-free mixtures and highly favorable performance for those made from mixtures reinforced with steel fibers.

The sample prepared using mix design M1 experienced the first visible crack after 3 blows in curing methods 1 and 2 and after 4 blows in curing method 3. These findings highlight the weakness of plain mixtures (without fibers) in the impact resistance test. Moreover, comparing the performance of mixtures across different curing methods reveals no significant effect of curing methods on the first crack resistance parameter. Specifically, the first crack resistance of the control mixture in curing methods 1 and 2 was identical, while in curing method 3, it increased by just one additional blow. Analyzing and comparing the behavior of other mixtures cured using different methods also indicate

that curing method variations do not significantly alter the impact resistance performance of the mixtures.

Additionally, the results confirm that the curing method does not influence the first crack impact resistance of the specimens. However, examining the impact resistance of specimens prepared with mixtures reinforced with steel fibers reveals a significant effect of these fibers in improving the impact properties of the specimens. The first crack resistance of mix design M1 in curing methods 1, 2, and 3 was 3, 3, and 4 blows, respectively. In contrast, adding 0.5% steel fibers by volume in mix design M2 increased this parameter to 42, 51, and 47 blows for curing methods 1, 2, and 3, respectively. Increasing the steel fiber content to 1% by volume further enhanced the first crack impact resistance to 69, 67, and 75 blows for curing methods 1, 2, and 3, respectively.

The comparison of other steel fiber-reinforced mix designs with similar fiber-free mixtures also highlights the significant positive role of steel fibers in improving the impact performance of reactive powder concrete (RPC) specimens. As the fiber content increases, the first crack impact resistance increases significantly. Observations showed that steel fibers, by bridging the cracks formed in disc-shaped specimens, prevent brittle failure, which is commonly observed in specimens produced with non-reinforced mixtures. Factors influencing the effectiveness of steel fibers include their tensile strength, embedded length within the matrix, and the surface roughness of the fibers, which enhances bonding with the matrix.

Polypropylene fibers also improved the first crack impact resistance of the specimens; however, their effect was considerably lower compared to steel fibers. A comparison of the first crack resistance of specimens prepared with mix designs M4 and M5 supports this conclusion. The sample prepared with mix design M4 (containing 1% polypropylene fibers) experienced first crack resistance values of 15, 14, and 14 blows for curing methods 1, 2, and 3, respectively. In contrast, the sample prepared with mix design M5 exhibited first crack impact resistance values of 21, 18, and 24 blows for curing methods 1, 2, and 3, respectively. Although these results demonstrate a significant improvement compared to the first crack impact resistance of the control mix, the improvement is substantially lower than that achieved by steel fibers.

Furthermore, the results indicate that another contributing factor to the improvement of the first crack impact resistance of RPC specimens is the amount of nano-silica used. Mix designs M2, M7, and M12 contain 0%, 0.5%, and 1% nano-silica, respectively, while all other properties remain the same. The results reveal that mix design M2 achieved first crack impact resistance values of 42, 51, and 47 blows across the three curing methods. In contrast, mix design M7 achieved values of 53, 66, and 56 blows, and mix design M12 achieved values of 63, 65, and 59 blows across the three curing methods. These results confirm the positive effect of nano-silica particles in enhancing the first crack impact resistance of the specimens.

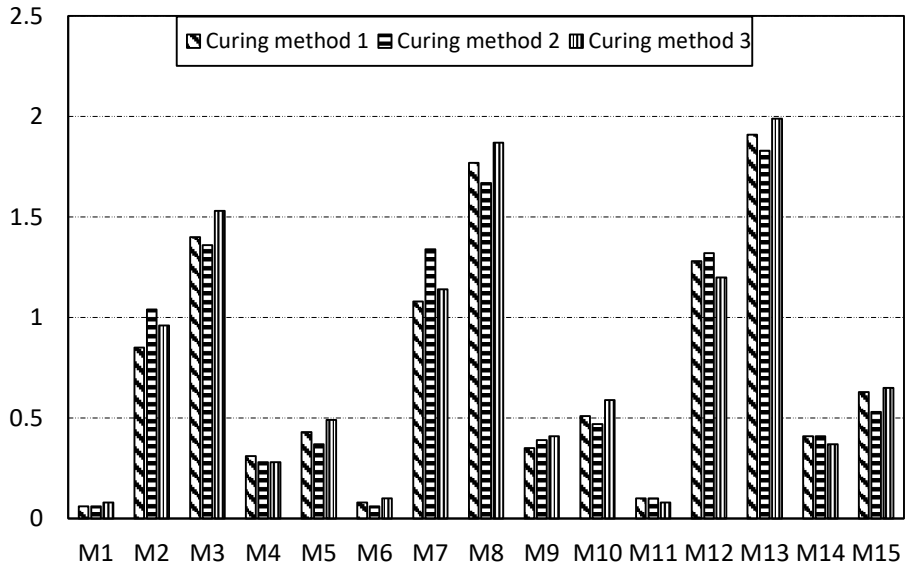

Figure 7. Energy absorption up to the occurrence of the first visible crack.

4.2.2. Ultimate Impact Resistance

The number of blows required to reach ultimate failure in the specimens was recorded, and based on this, the absorbed energy was determined. The results for this parameter, expressed in kilojoules (kJ), are shown in Figure 8. The number of blows sustained after the first visible crack until ultimate failure serves as an indicator of the ductility and toughness of the specimen in the impact resistance test.

The results for ultimate impact resistance, similar to those of first crack resistance, indicate poor performance for the fiber-free mixtures and favorable performance for mixtures reinforced with steel fibers. The specimen prepared using the control mix (without fibers and nano-silica) experienced ultimate failure after 4 blows in curing method 1 and after 5 blows in curing methods 2 and 3. These results indicate that after the first visible crack appeared in the fiber-free mixtures, the specimens reached ultimate failure rapidly, exhibiting brittle failure with no secondary resistance.

Moreover, the results demonstrate that the curing method does not significantly influence the ultimate impact resistance of the specimens. A comparison of the mixtures across different curing methods reveals no substantial effect of the curing method on the ultimate impact resistance parameter. For example, the ultimate impact resistance of the control sample in curing methods 1, 2, and 3 was 4, 5, and 5 blows, respectively, indicating negligible variation. Similarly, evaluating the behavior of other mixtures cured using different methods confirms that changes in the curing method do not result in significant differences in ultimate impact resistance.

The test results further revealed that, unlike fiber-free mixtures, the steel fiber-reinforced mixtures sustained a considerable number of additional blows after the first crack before reaching ultimate failure. Therefore, steel fibers effectively bridged the cracks in the concrete discs, preventing their propagation and delaying ultimate failure. This improved the toughness and ductility of the specimens in the impact resistance test.

The ultimate impact resistance values for mix designs M1, M2, and M3 under curing method 1 were 4, 89, and 136 blows, respectively, while for curing method 2, they were 5, 102, and 147 blows, and for curing method 3, they were 5, 101, and 152 blows, respectively. These mixes were identical in composition except for the steel fiber content, with mix M1 containing no fibers, mix M2 containing 1% steel fibers by volume, and mix M3 containing 2% steel fibers by volume. These results clearly demonstrate the significant positive impact of steel fibers on improving the ultimate impact resistance of the specimens.

A comparison of other steel fiber-reinforced mix designs with their fiber-free counterparts further confirms the enhancement in ultimate impact resistance due to steel fibers. The results also indicate that as the fiber content increases, the ultimate impact resistance improves considerably.

The impact resistance evaluation of specimens prepared with polypropylene fiber-reinforced mixtures also demonstrated the positive role of these fibers in enhancing ultimate impact resistance. However, their effect was significantly lower compared to steel fibers. A comparison of the ultimate impact resistance of samples made with mix designs M4 and M5, which contain 1% and 2% polypropylene fibers, respectively, confirms this conclusion. The specimen prepared with mix M4 experienced ultimate impact resistance values of 19, 21, and 20 blows for curing methods 1, 2, and 3, respectively. In contrast, the specimen prepared with mix M5 achieved values of 32, 31, and 39 blows for curing methods 1, 2, and 3, respectively. Although these results show a relatively significant improvement in ultimate impact resistance compared to fiber-free samples, this improvement is considerably lower than that observed with steel fibers.

Additionally, the amount of nano-silica used in the samples was identified as another influential factor in the ultimate impact resistance of the mixtures. Mix designs M2, M7, and M12 contain 0%, 0.5%, and 1% nano-silica, respectively, with all other properties remaining the same. The results indicate that mix M2 achieved ultimate impact resistance values of 89, 102, and 101 blows across the three curing methods, while mix M7 achieved values of 99, 112, and 107 blows, and mix M12 achieved values of 140, 135, and 129 blows. These results suggest a positive, though not highly significant, effect of nano-silica particles in enhancing the ultimate impact resistance of the specimens.

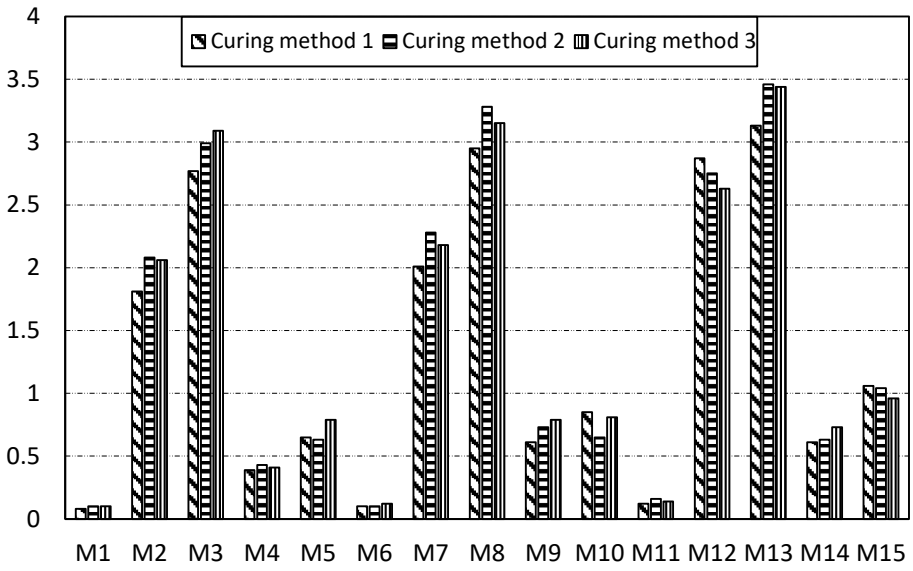

Figure 8. Energy absorption up to the point of ultimate failure.

4.3. Statistical Analysis of Results

Over the past few decades, various probabilistic models have been proposed for the statistical analysis of concrete impact resistance. The effectiveness of the two-parameter Weibull distribution in this context has been validated by several researchers (Li et al., 2007; Raif & Irfan, 2008). Therefore, in this study, the two-parameter Weibull distribution was utilized for the statistical analysis of drop-weight impact test results using the graphical method [22]. The cumulative distribution function F(n) of the two-parameter Weibull probability law is expressed in terms of the probability density function, as shown in Equation 4 [23]:

4) $F(n) = 1 - exp[-(n/u)^{\alpha}]$

Where:

- n is the impact resistance of concrete,
- alpha is the Weibull shape parameter,
- u is the scale parameter.

The function F(n) represents the probability of failure. Thus, the survival probability function is given by Equation 5:

5) $L(n) = 1 - F(n) = exp[-(n/u)^{\alpha}]$

Taking the natural logarithm twice on both sides of Equation 5 results in Equation 6:

6) $\ln\ln(\frac{1}{L(n)}) = \alpha \ln(n) - \alpha \ln(u)$

As shown in Equations 7 and 8, Equation 6 represents a linear relationship between ln ln(1/L(n)) and ln(n):

7) $Y = \ln\ln(\frac{1}{L(n)}), X = \ln(n), \beta = \alpha \ln(u)$

8) $Y = \alpha X - \beta$

The empirical survival function L(n) for the impact test data was obtained using Equation 9 [24-27]:

9) $L(n) = 1 - \frac{i}{1+k}$

Where:

- i is the order number of the tested samples (i = 1, 2, 3, 4),
- k is the total number of impact samples for a specific group.

Using this method, a plot between X and Y was drawn based on Equation 8. If a linear relationship exists between X and Y, the method is considered a suitable statistical approach for describing the first crack resistance (N1) and ultimate resistance (N2).

From the regression equations obtained through the linear relationship between X and Y, the coefficients alpha and beta in Equation 7, along with the coefficient of determination (R^2), were calculated. The statistical analysis results for first crack resistance (N1) and ultimate resistance (N2) for all mix designs are presented in Figure 9 and Figure 10. Additionally, the values of alpha, beta, and R^2 for the parameters N1 and N2 are shown in Table 4.

All obtained values for the coefficient of determination (R^2) exceeded 0.90, indicating that the two-parameter

Weibull distribution is an appropriate method for the statistical analysis of the impact resistance of reactive powder concrete.

Table 4. Linear regression results of impact resistance tests using the Weibull statistical distribution.

Index	Mix Design	alpha	beta	R^2	Index	Mix Design	alpha	beta	R^2
N1	M1	4.88	-8.25	0.919	N2	M1	4.21	-7.37	0.922
	M2	20.39	-65.46	0.925		M2	7.13	-28.33	0.967
	M3	18.14	-66.07	0.989		M3	14.99	-69.33	0.985
	M4	9.04	-28.55	0.989		M4	10.58	-44.69	0.987
	M5	2.40	-4.08	0.921		M5	2.91	-6.67	0.978
	M6	15.68	-54.89	0.988		M6	4.25	-18.22	0.934
	M7	17.79	-51.85	0.915		M7	6.25	-23.95	0.952
	M8	13.54	-50.11	0.932		M8	6.59	-30.76	0.945
	M9	5.07	-9.69	0.923		M9	4.36	-11.14	0.908
	M10	15.81	-44.27	0.915		M10	6.68	-24.71	0.957
	M11	12.35	-40.17	0.916		M11	10.79	-47.70	0.923
	M12	4.88	-8.25	0.920		M12	2.95	-5.53	0.918
	M13	7.59	-26.41	0.951		M13	11.72	-53.38	0.965
	M14	2.13	-3.00	0.997		M14	2.84	-5.45	0.920
	M15	4.27	-11.26	0.970		M15	9.98	-37.16	0.954

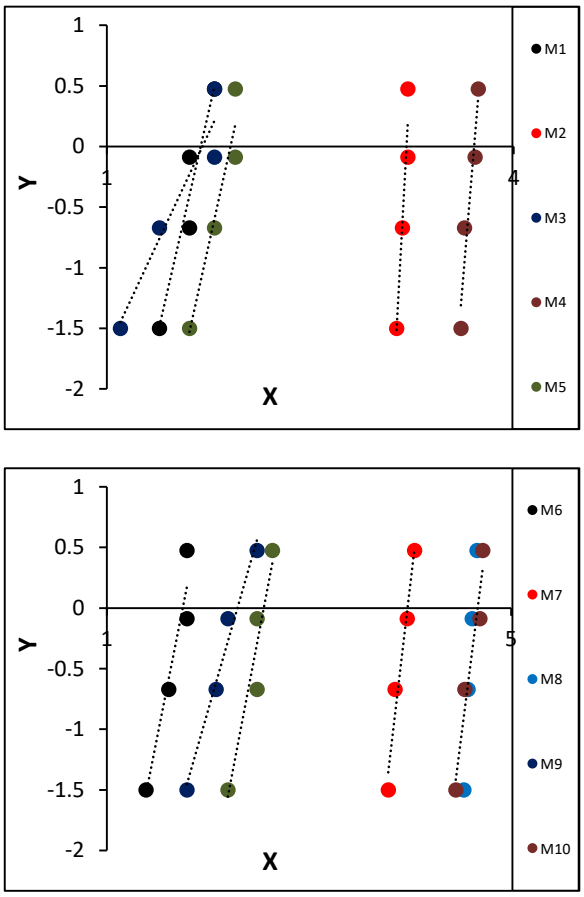

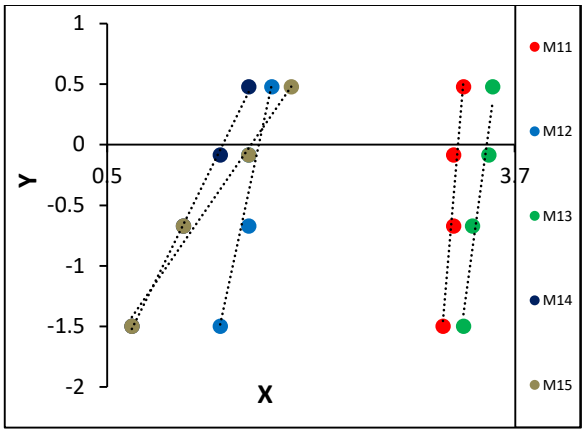

Figure 9. Linear regression of first crack resistance (N1) using the Weibull distribution.

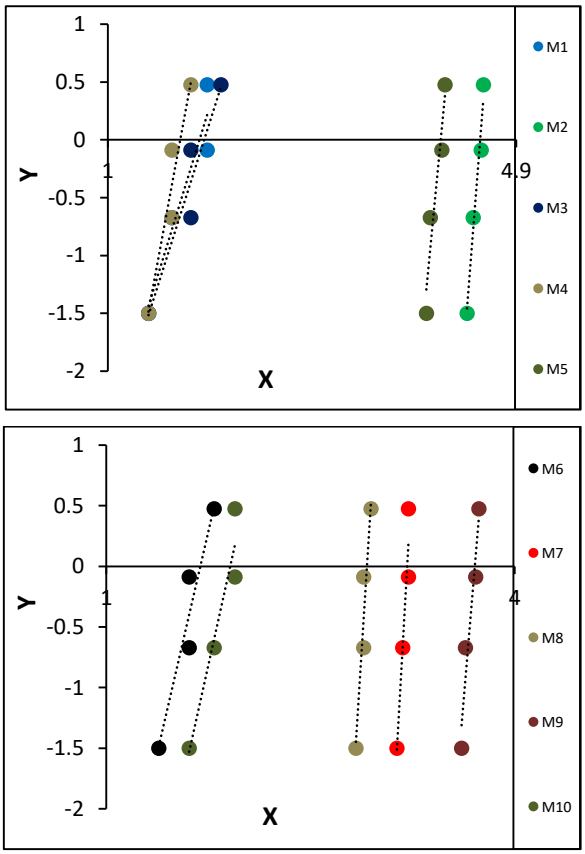

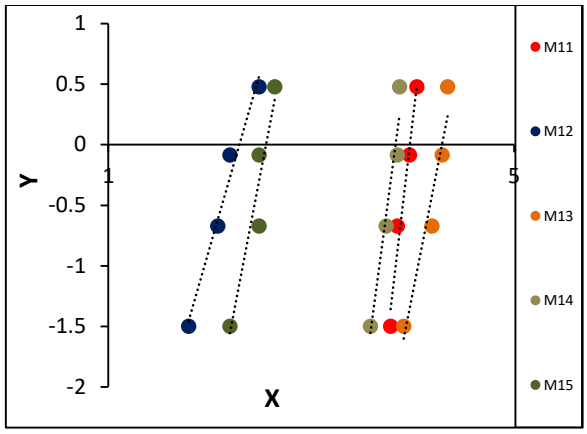

Figure 10. Linear regression of ultimate resistance (N2) using the Weibull distribution.

5. Discussion and Conclusion

This study investigated the compressive strength and impact properties of reactive powder concrete (RPC). The RPC mixtures examined in this research contained nano-silica and were reinforced with steel and polypropylene fibers, subjected to three different curing methods. Nano-silica was incorporated at levels of 0%, 0.5%, and 1% by weight of cement in the sample preparation. Additionally, the mixtures were reinforced with steel and polypropylene fibers at volume fractions of 0%, 1%, and 2%. Three curing methods were employed: standard moist curing for 28 days, thermal curing in hot water at 90°C for 2 days followed by moist curing until the age of 28 days, and thermal curing in hot water at 90°C for 5 days followed by moist curing until the age of 28 days. The impact resistance test was conducted using the repeated drop-weight impact method, and parameters such as first crack resistance, ultimate resistance, and energy absorption were analyzed. The key findings of the study are summarized as follows:

Steel fibers exhibited dual behavior in the compressive strength test. Specifically, at a volume fraction of 1%, they improved compressive strength, whereas at 2%, they caused a reduction in compressive strength. Therefore, steel fibers should be used at an optimal dosage in the production of RPC mixtures.

Polypropylene fibers did not significantly influence the compressive performance of the mixtures, whereas thermal curing and nano-silica enhanced the compressive strength. Thermal curing for 5 days resulted in a 48% increase in compressive strength, while the incorporation of 1% nano-silica led to a 54% improvement.

The impact resistance test results indicated a significant influence of steel fibers and a lesser effect of polypropylene fibers in enhancing the impact resistance of the specimens. Specifically, the addition of 2% steel fibers increased the ultimate impact resistance from 4 blows in the control sample to 136 blows, whereas the same volume fraction of polypropylene fibers increased this parameter to only 32 blows.

The curing method and nano-silica content also contributed to improving the impact performance of the specimens to some extent. It was observed that longer thermal curing durations and higher nano-silica content led to improved impact performance.

Statistical analysis of the impact resistance test results demonstrated that the two-parameter Weibull distribution is an appropriate statistical model for analyzing the impact resistance of RPC.

The findings of this study indicate that by optimizing the use of nano-silica, steel fibers (especially steel fibers), and thermal curing methods, RPC with significantly high compressive and impact resistance can be achieved. These concretes have great potential for application in high-performance structures.

Authors' Contributions

Authors equally contributed to this article.

Acknowledgments

Authors thank all participants who participate in this study.

Declaration of Interest

The authors report no conflict of interest.

Funding

According to the authors, this article has no financial support.

Ethical Considerations

All procedures performed in this study were under the ethical standards.

References

[1] W. Kurdowski, A. Garbacik, and H. Szelag, "The influence of reactive powder types on the properties of concrete of reactive powders," *Cem. Wapno, Bet*, vol. 29, pp. 292-300, 2009.

[2] O. A. Mayhoub, A. R. El-Sayed, and A. Yehia, "Behavior of RPC based Alkali Activated Material Compared with Conventional RPC," *Int. J. Innov. Technol. Explor. Eng*, vol. 9, pp. 562-567, 2020.

[3] O. A. Mayhoub, E. S. Nasr, Y. A. Ali, and M. Kohail, "The influence of ingredients on the properties of reactive powder concrete: A review," *Ain Shams Eng J*, vol. 36, pp. 145-257, 2020, doi: 10.1016/j.asej.2020.07.016.

[4] W. Huang, "The Relationship Between Construction Workers' Emotional Intelligence and Safety Performance," *Engineering Construction & Architectural Management*, vol. 31, no. 5, pp. 2176-2201, 2024, doi: 10.1108/ecam-07-2023-0747.

[5] N. Ishak, "Elucidation of the Influence of Construction Waste Causative Factors and Strategies Towards Sustainable Construction Waste Management Improvement," *Iop Conference Series Earth and Environmental Science*, vol. 1303, no. 1, p. 012040, 2024, doi: 10.1088/1755-1315/1303/1/012040.

[6] M. V. Kumar, "A Review on Sustainable Construction," *International Journal of Research and Review*, vol. 11, no. 4, pp. 251-258, 2024, doi: 10.52403/ijrr.20240427.

[7] A. Maher El-Tair, M. S. El-Feky, K. G. Sharobim, H. Mohammedin, and M. Kohail, "Improving the reactivity of clay nano-particles in high strength mortars through indirect sonication method," *Int. J. Sci. Technol. Res*, vol. 9, pp. 1045-1054, 2020.

[8] C. M. Tam, V. W. Y. Tam, and K. M. Ng, "Optimal conditions for producing reactive powder concrete," *Mag. Concr. Res*, vol. 62, pp. 701-716, 2010, doi: 10.1680/macr.2010.62.10.701.

[9] J. Dugat, N. Roux, and G. Bernier, "Mechanical properties of reactive powder concretes," *Mat. Struct*, vol. 29, pp. 233-240, 1996, doi: 10.1007/BF02485945.

[10] S. Abbas, M. L. Nehdi, and M. A. Saleem, "Ultra-high performance concrete: Mechanical performance, durability, sustainability and implementation challenges," *Int. J. Concr. Struct. Mater*, vol. 10, pp. 271-295, 2016, doi: 10.1007/s40069-016-0157-4.

[11] C. Wang, C. Yang, F. Liu, C. Wan, and X. Pu, "Preparation of Ultra-High Performance Concrete with common technology and materials," *Cem. Concr. Compos*, vol. 34, pp. 538-544, 2012, doi: 10.1016/j.cemconcomp.2011.11.005.

[12] M. S. El-Feky, M. Kohail, A. M. El-Tair, and M. I. Serag, "Effect of microwave curing as compared with conventional regimes on the performance of alkali activated slag pastes," *Constr. Build. Mater*, vol. 233, p. 117268, 2020, doi: 10.1016/j.conbuildmat.2019.117268.

[13] C. Shang *et al.*, "Investigating mechanical properties and microstructure of reactive powder concrete blended with sulfoaluminate cement," *Case Studies in Construction Materials*, vol. 17, p. 01552, 2022, doi: 10.1016/j.cscm.2022.e01552.

[14] ASTM, "ASTM C150, Standard Specification for Portland Cement," 2012.

[15] ASTM, "ASTM C39, Standard Test Method for Compressive Strength of Cylindrical Concrete Specimens," 2003.

[16] E. Negahban, A. Bagheri, and J. Sanjayan, "Pore structure profile of ambient temperature-cured geopolymer concrete and its effect on engineering properties," *Construction and Building Materials*, vol. 406, p. 133311, 2023, doi: 10.1016/j.conbuildmat.2023.133311.

[17] V. Afroughsabet, L. Biolzi, and T. Ozbakkaloglu, "Influence of double hooked-end steel fibers and slag on mechanical and durability properties of high performance recycled aggregate concrete," *Composite Structures*, vol. 181, pp. 273-284, 2017, doi: 10.1016/j.compstruct.2017.08.086.

[18] A. Sahraei Moghadam, F. Omidinasab, and A. Dalvand, "Experimental investigation of (FRSC) cementitious composite functionally graded slabs under projectile and drop weight impacts," *Construction and Building Materials*, vol. 237, p. 117522, 2020, doi: 10.1016/j.conbuildmat.2019.117522.

[19] L. I. Gong, X. Yu, Y. Liang, X. Gong, and Q. Du, "Multi-scale deterioration and microstructure of polypropylene fiber concrete by salt freezing," *Case Studies in Construction Materials*, vol. 18, p. 01762, 2023, doi: 10.1016/j.cscm.2022.e01762.

[20] C. Herath, D. W. Law, C. Gunasekara, and S. Setunge, "Sulphate and acid resistance of HVFA concrete incorporating nano silica," *Construction and Building Materials*, vol. 392, p. 132004, 2023, doi: 10.1016/j.conbuildmat.2023.132004.

[21] P. Hou, X. Wang, X. Zhou, X. Cheng, and S. P. Shah, "Regulations on the hydration, morphology, and sulfate-attack resistivity of C3A with micro/nano-silica particles," *Construction and Building Materials*, vol. 324, p. 126388, 2022, doi: 10.1016/j.conbuildmat.2022.126388.

[22] S. Goel, S. P. Singh, and P. Singh, "Fatigue analysis of plain and fiber-reinforced self-consolidating concrete," *ACI Materials Journal*, vol. 109, pp. 573-582, 2012, doi: 10.14359/51684089.

[23] Y. Ding, D. Li, Y. Zhang, and C. Azevedo, "Experimental investigation on the composite effect of steel rebars and macro fibers on the impact behavior of high performance self-compacting concrete," *Construction and Building Materials*, vol. 136, pp. 495-505, 2017, doi: 10.1016/j.conbuildmat.2017.01.073.

[24] H. Li, M. Zhang, and J. Ou, "Flexural fatigue performance of concrete containing nanoparticles for pavement," *International Journal of Fatigue*, vol. 29, pp. 1292-1301, 2007, doi: 10.1016/j.ijfatigue.2006.10.004.

[25] J. Li, K. Zhang, and Z. Deng, "Distribution regularity of flexural impact resistance of synthetic macro-fiber reinforced concrete," *Journal of Architectural Engineering*, vol. 24, pp. 54-59, 2007.

[26] M. Mastali, A. Dalvand, A. R. Sattarifard, Z. Abdollahnejad, and M. Illikainen, "Characterization and optimization of hardened properties of self-consolidating concrete incorporating recycled steel, industrial steel, polypropylene and hybrid fibers," *Composites Part B*, vol. 151, pp. 186-200, 2018, doi: 10.1016/j.compositesb.2018.06.021.

[27] L. Wang, H. Wang, and J. Jia, "Impact resistance of steel-fibre-reinforced lightweight-aggregate concrete," *Magazine of Concrete Research*, vol. 67, pp. 539-547, 2009, doi: 10.1680/macr.2007.00128.